

SUPPLEMENTARY METHODS AND DATA

1 SUPPLEMENTAL MATERIALS AND METHODS

1.1 Study of virus sequence evolution

Amplicon Design: Primer landing sites were identified in regions of high conservation around the anti-sense target region with the help of Primer3 program (<http://primer3.sourceforge.net/>). Primer sequences are shown in Table S1.1 and are named per the schema provided in Figure 4A. Primers were labeled with DNA barcodes to enable multiplex pyrosequencing of samples.^{40,41}

Sample Preparation for Pyrosequencing: Total RNA was extracted from plasma samples for each patient/time-point combination listed in Table S4 and S5 using the *Illustra* RNAspin kit (GE Healthcare, Buckinghamshire, UK). For efficient extraction, RNA carrier was used. HIV RNA was reverse-transcribed and amplified with *One-step* RT-PCR (Qiagen, Valencia, CA) and using *RNasin* RNase inhibitor (Promega, Madison, WI). A touchdown protocol was used: 1 x (30 min at 50°C), 1 x (15 min at 95°C), 10 x (1 min at 94°C; 1 min at 58°C-53°C, 0.5°C iterative decrement; 1 min at 72°C) (starting with a temperature of 58°C and reducing it successively by 0.5°C to reach 53°C), 25 x (1 min at 94°C; 1 min at 53°C; 1 min 15 sec at 72°C), 1 x (10 min at 72°C; maintained at 4°C). PCR products were purified using Agencourt AMPure XP (Beckman Coulter). DNA was quantified and pooled and then analyzed by 454/Roche pyrosequencing.

Pyrosequence data processing for the analysis of genetic pressure: Two amplicons covering the antisense-target region and flanking non-target regions were pyrosequenced in both directions. Reads were filtered for quality, assigned to source samples and de-noised using Pyronoise.^{42,43} Pyronoise groups reads into clusters, here termed operational taxonomic units (OTUs), which are representative of the different viral variants sequenced. The predominant sequence isolated from a patient was used to obtain pair-wise alignments (PWAs) for all de-noised OTUs for that patient. Multiple sequence alignments (MSAs) were constructed for each patient from the respective PWA sets. MSA positions with low read coverage (<5%) were discarded from subsequent analysis. Departures from the MSA consensus were scored as base changes and deletions. Sequence reads were stored in a MySQL database and analyzed using custom programs in R. Analytical software is available upon request.

Table S1.1. Primer sequences used – named as shown in main text Figure 4A				
	Coordinates		Sequence	
	From	To	454 Adapter	HIV template specific part
1F	6432	6451	GCCTCCCTCGCGCCATCAG	CACATGCCTGTGTACCCACA
1R	7017	6994	GCCTTGCCAGCCCGCTCAG	TCTTCTGCTAGACTGCCATTTAAC
2F	6993	7016	GCCTCCCTCGCGCCATCAG	TGTTAAATGGCAGTCTAGCAGAAG
2R	7639	7618	GCCTTGCCAGCCCGCTCAG	CATATCTCCTCCTCCAGGTCTG

1.2 Integration site analysis

Genomic DNA was extracted from PBMCs using the Invitrogen Dynabeads MyPure CD4 Kit 2 to enrich for CD4+ T cells and the Qiagen DNeasy Blood and Tissue kit for DNA extraction. To introduce PCR adapters, DNA was treated separately with MuA transposase⁴⁴ or one of three restriction enzyme/ligase combinations (*ApoI*, *NspI*, or a cocktail of *AvrII/Spel/NheI*). PCR was carried out as described previously⁴⁵ using primers specific for a unique sequence (GTAG) present in the VRX496 vector and for the PCR linker. PCR products were diluted and nested PCR with primers specific for the LTR and linker was then performed. Amplification products were sequenced on a 454 pyrophosphate sequencing platform using Titanium chemistry. DNA Barcodes present in the nested second round PCR primers allowed multiplexing of amplicons for sequencing.^{45,46}

Sequences having a single best hit with $\geq 98\%$ identity to the human genome (hg18, version 36.1), aligning within three base pairs of the beginning of the sequence read, and containing the terminal LTR sequence TCTAGCA between the LTR primer and the site of integration were counted as true integration events. Comparisons of integration site distributions to those of genomic features were carried out using logistic regression as described previously.^{47,48} Computationally selected random genomic sites (matched random controls that are constrained to lie the same distance from a restriction enzyme cleavage site as the paired experimental integration site) were used for comparison. Gene expression analysis was based on microarray data from Jurkat cells measured using the Affymetrix HU133 plus 2.0 gene chip array.⁴⁹ The Cancer-gene list used is at (<http://microb230.med.upenn.edu/protocols/cancergenes.html>). All sequences will be deposited in the SRA repository upon acceptance of this manuscript for publication.

1.3 Rectal biopsies

Prior to biopsy, patients were prepped with a fleet enema and then were offered a short acting benzodiazepine prior to the procedure. Pinch biopsies were performed using 6 passes with a two-pronged forceps to obtain a total of 12 biopsies. 9 biopsies are used for intraepithelial lymphocytes (IEL) collection, and the remaining biopsies are formalin fixed or undergo whole tissue DNA isolation for look back purposes. Biopsies used for IEL isolation were placed in 90% RPMI supplemented w/10% heat-activated fetal bovine serum and 1% 100x penicillin streptomycin for overnight or same day delivery at 4°C to the Human Immunology Core at the University of Pennsylvania IEL isolation. The IEL were isolated using a protocol derived from Shacklett et al.⁵⁰ With 9 biopsies, approximately 1.5- 2 million IELs are obtained, after Percoll gradient (GE Life Sciences). One portion of the IELs was stained for CD3/CD4/CD8 by flow cytometry to obtain a total percentage of CD4 T cells in the IEL preparation, and the remainder of the cells was utilized to quantify VRX496 proviral copies. Isolated IEL were suspended in DNA lysing buffer (100 mM KCl; 0.1% NP40; 20 mM Tris pH 8.4; 0.5 mg/ml proteinase K). Quantification by realtime PCR was carried out on 20,000 IEL in duplicate reactions using primers/probe sets as described below, with a lower limit of quantification of 200 copies per 10e6 IEL.

1.4 Persistence, conditional replication assays, and VSV-G antibody

Subject's blood was collected by using Vacutainer Cell Preparation Tubes (CPTs; BD Biosciences) and centrifuged following manufacturer's recommendations. Plasma and mononuclear cells were recovered from CPTs and centrifuged. Plasma was recovered within 24 hours and frozen whereas mononuclear cells were washed twice in PBS (BioWhittaker) before being dry pelleted and frozen.

For detection of mobilized VRX496 lentiviral vector, 1.5 milliliters of frozen subject's plasma were thawed and processed with Qiagen's MinElute kit following manufacturer's recommendation. Five microliters of eluted RNA per well, 45 replicates per sample, were used for one round of amplification (40 cycles) by real-time RT-PCR (ABI Prism 7900). Primers used for detecting Gtag sequence were 5'-TGC-AGA-AGA-AGC-GCA-TCA-AG-3' and 5'-GTG-TTC-TGC-TGG-TAG-TG-3'. Results were reported as number of mobilized VRX496 copies per ml of plasma.

For detection of vector modified cells, three 10e6 mononuclear cell-containing frozen dry pellets were thawed and processed by using Qiagen's M48 automated DNA purification device with the MagAttract DNA kit following manufacturer recommendations. Eluted DNA concentration was assessed by using Picogreen Kit (Molecular Probes/Invitrogen) following manufacturer's recommendation on a BioTek Synergy HT microplate reader. Twenty five thousand cells of genomic DNA equivalent was used for one round of amplification (40 cycles) by real-time PCR (ABI Prism 7900). Primers used for detecting Gtag

sequence were 5'-AGA-AGA-ACG-GCA-TCA-AGG-TGA-A-3' and 5'-GGA-CTG-GGT-GCT-CAG-GTA-GTG-3'. Results were reported as number of VRX496 copies per million of mononuclear cells. An ELISA kit (VSVg #5433) was specially developed by Advanced BioScience Laboratories, Inc. (ABL). For the generation of anti-VSV-G antibodies as an assay positive control, three subcutaneous infusions were administered to a single non-human primate monkey with 2 mL of inactivated VRX496™ (lot VRX496Exp03) mixed with an adjuvant and boosted with an injection of VSV-G protein obtained from Sigma. ELISA plates were coated with protein lysate from human embryonic kidney cells (HEK293) previously transfected with a plasmid construct expressing VSV-G. Test articles were determined to be positive if their optical density (OD) values were greater than the OD value of the negative control plus five standard deviations. Potential subjects were tested according to the VSV-G ELISA procedure during the screening process. If a subject's plasma tested positive at screening, he/she was not eligible to enroll in the clinical studies. Enrolled subjects were subsequently tested for anti-VSV-G antibodies following infusion(s) according to scheduled time-points set forth in the Lexgenleucel-T clinical protocols.

1.5 Detection of HIV specific immune responses

To measure of anti-HIV antigen-responses in patient PBMC, we evaluated the presence of anti-HIV immune responses in peripheral blood mononuclear cells of patients collected pre-T cell infusion and at approximately 10 week post STI by multi-parametric flow cytometry using CD107a and intracellular detection of IFN- γ and MIP1- β using intracellular cytokine secretion (ICS) assays. For these experiments, autologous patient PBMC collected prior to treatment were transduced to express all HIV antigens except env using the VRX1169 vector, which contains a 119 base pair deletion of the HIV env gene and is pseudotyped to VSV-G. VRX1169-transduced PBMC were subsequently labeled with CFSE and used as targets against patient PBMC at an E:T ratio of 0.2:1. Prior to analysis the gating strategy excluded infected target cells (CFSE-positive), and dead cells, followed by a positive gate on CD3+ cells. As summarized in Table S10, no significant HIV antigen-specific activity was detected in any of the patient samples by either degranulation or ICS assays.

1.6 Statistics

The majority of methods for statistical analysis are detailed in the body of the main manuscript. To establish the half-life of VRX496-T, one- and two-phase exponential decay models on log transformed data were evaluated. Least square estimates were used to fit the non-linear equations. The comparison of the model were determined by generalized F-test and AIC. Confidence intervals were calculated after adjusting for possible cluster effects due to longitudinal measures from the same subject over time. Separate analyses were done for the 6- and 3-infusion groups. As reported in the main text of this

manuscript, there was no significant difference in persistence of VRX496-T in patients receiving 6 versus 3 infusions, using a single stage decay curve (Figure 5). However, for patients receiving the 6 infusions, a two stage decay curve could be fit, whereas the 3 infusion cohort only had a single stage decay curve. This may be a result of insufficient data in the 3 infusion cohort to fit a two stage model, or it could represent a true difference illustrating accelerated initial decay of VRX496-T in patients receiving the 6 infusions. In the two stage model, the second stage begins at 6.65 weeks post infusion.

2 SUPPLEMENTAL DATA

Table S1A. Absolute viral load summaries for patients infused on the 6 dose protocol

Timepoint	Study Day	Absolute Viral Load (copies per mL of blood)												
		201	202	203	204	206	207	208	209	211	212	213	214	215
Screen	Screen	0	0	0	0	0	0	0	0	0	0	0	0	0
Week -2	Safety	0	96	0	0	0	0	0	0	0	0	0	0	0
Day 0	Dose 1	0	0	0	0	0	105	65	129	0	0	659	0	0
Week 1	Safety	0	0	0	0	481	0	0	0	0	0	76	0	0
Week 2	Dose 2	NA	NA	NA	NA	NA	NA	NA	NA	NA	NA	NA	NA	NA
Week 3	Safety	0	59	0	0	0	0	0	0	0	0	93	102	0*
Week 4	Dose 3	NA	NA	NA	NA	NA	NA	NA	NA	NA	NA	NA	NA	NA
Week 5	Safety	95	73	0	0	0	0	0	0	0	0	0	0	0
Week 6	Safety	0	0	0	0	0	0	110	0	0	0	54	0	0
Week 8	Safety	0	0	0	0	0	0	0	0	0	0	0	0	0
Week 9	Dose 4	0	0	0	0	0	0	0	0	0	0	76	NA**	0
Week 10	Safety	0	0	0	0	137	58	0	123	0	0	53	NA**	0
Week 11	Dose 5	0	401	0	0	878	88	0	66	0	0	0	NA**	0
Week 12	Safety	0	0	75	0	145	0	52	0	0	0	0	NA**	0
Week 13	Dose 6	0	0	111	0	0	0	0	0	0	0	0	NA**	0
Week 14	Safety	0	0	0	0	0	Invalid assay	83	0	0	0	Missed	93	0
Week 16	Safety	0	0	0	0	102	0	0	0	0	0	Missed	0	0
Week 18	STI	0	0	0	0	0	0	0	0	0	0	NA	0	0
Week 20	Safety	396	76	2325	189	8110	>100000	NA	NA	NA	516	NA	1758	0
Week 22	Safety	31446	46886	62443	5938	>100000	1065	NA	NA	NA	25193	NA	44856	0
Week 24	Safety	31077	61589	39524	26627/ >100000	9689	1727	0	0	0	123,117	0	8789	1356
Week 28	Safety	46020	62630	26925	5993	5970	787	NA	NA	NA	39686	NA	257	2488
Week 32	Safety	29520	294	11651	17083	3042	81	NA	NA	NA	25939	NA	345	6014
Week 36	Safety	28174	68	18463	22108	1150	52	0	0	0	636	0	0	3360
Week 40	Safety	29819	292	14907	22673	2144	125	NA	NA	NA	1518	NA	0*	3806
Week 44	Safety	18684	0	8049	20650	242	Missed	NA	NA	NA	240	NA	0	4522
Week 48	Safety	44531	0	8710	17022	52	120	NA	NA	NA	101	NA	0	4690
Week 52	Safety	33467	116	26563	16940	294	151	0*	0*	0	54	0	0	3952

Viral Load values in **bold** print are those obtained while subject was not on ARVs.
 *Patient had an HIV-1 RNA viral load below the Limit of Quantification for this assay (48 copies/mL), but above the lower Limit of Detection for the test. Because of the low viral load, actual level of the virus in the patient's sample could not be determined accurately.
 **Subject VRX496-214 did not have 2nd cycle of dosing of VRX496 (doses 4-6). QC testing of RCL by VIRxSYS, testing required and requested by the FDA delayed dose #4 by 6 weeks. In light of delay, team decided and protocol deviation approved to have subject proceed to STI after receiving 3 doses of VRX496 instead of 6 as stipulated in the protocol version in which subject was enrolled. Subject had Weeks 14 and 16 safety evaluations and then proceeded to Week 18, STI.

Table S1B. Absolute viral load summaries and analysis for subjects enrolled in protocol versions 1.12 or 1.13

Timepoint	Study Day	Absolute Viral Load (copies per mL of blood)			
		218	250	251	252
Screen	Screen	0	0	0	0
Week -2	Safety Labs	0*	0	0	0
Day 0	Dose 1	0*	0	0	0
Week 1	Safety Eval	0*	0	0	0
Week 2	Dose 2	NA	NA	NA	NA
Week 3	Safety Eval	0	0	0	0
Week 4	Dose 3	NA	NA	NA	NA
Week 5	Safety Eval	Missed	0	0	0
Week 6	Safety Eval	0*	0	0	0
Week 8	Safety Eval	83	0	0	0
Week 10	STI	0	0	0	0
Week 12	Safety Eval	89	0	0	0
Week 14	Safety Eval	368	25076	34215	0
Week 16	Safety Eval	97623	414365	77545	0
Week 20	Safety Eval	15497	101458	10518	0
Week 24	Safety Eval	11366	78853	22639	0
Week 28	Safety Eval	28061	876	36921	5052
Week 32	Safety Eval	23525	387	605	57599
Week 36	Safety Eval	24588	0	99	365196
Week 40	Safety Eval	27398	79	55	309531
Week 44	Safety Eval	19508	0	92	Missed
Week 48	Safety Eval	Missed	0	0	Missed
Week 52	Safety Eval	1105	0	0	0

Viral Load values in **bold print** are those obtained while subject was not on ARVs.

Table S2. Viral load set points: reference clinical assay.

The test used for determination of viral load values, based on the source documents, is shown.

Patient	Date	VL	Reading	Test Used
201	29-Jul-04	47,707	historic	versant branched DNA
201	26-Aug-04	87,002	historic	versant branched DNA
201	7-Oct-04	70,558	historic	versant branched DNA
201	1-May-07	46,020	TI week 10	roche amplicor QNT PCR
201	31-May-07	29,520	TI week 14	roche amplicor QNT PCR
203	5-Sep-95	65,529	historic	Smith Kline Beecham PCR
203	28-Aug-07	26,925	TI week 10	roche amplicor QNT PCR
203	25-Sep-07	11,651	TI week 14	roche amplicor QNT PCR
204	2-Jun-98	110,000	historic	Smith Kline Beecham PCR
204	3-Dec-07	5,993	TI week 10	roche amplicor QNT PCR
204	2-Jan-08	17,083	TI week 14	roche amplicor QNT PCR
215	3-Dec-02	45,618	historic	Roche ultrasensitive PCR
215	16-Apr-09	2,488	TI week 10	Roche Cobas Taqman
215	14-May-09	6,014	TI week 14	Roche Cobas Taqman
218	11-Feb-00	10,359	historic	"HIV-1-RNA RT-PCR"
218	22-Jul-09	11,366	TI week 10	Roche cobas taqman
218	18-Aug-09	28,061	TI week 14	Roche cobas taqman
250	17-Jan-02	3,532	historic	cobas (Taqman) ampliprep
250	30-Apr-02	4,053	historic	cobas (Taqman) ampliprep
250	15-Oct-02	7,467	historic	cobas (Taqman) ampliprep
250	13-Feb-03	8,406	historic	cobas (Taqman) ampliprep
250	22-May-03	142,783	historic	cobas (Taqman) ampliprep
250	17-Jul-03	32,579	historic	cobas (Taqman) ampliprep
250	6-Nov-03	15,086	historic	cobas (Taqman) ampliprep
250	27-Jan-04	11,168	historic	cobas (Taqman) ampliprep
250	27-Apr-04	238,133	historic	cobas (Taqman) ampliprep
250	23-Jun-04	31,897	historic	cobas (Taqman) ampliprep
250	31-Aug-04	31,071	historic	cobas (Taqman) ampliprep
250	30-Nov-04	21,439	historic	cobas (Taqman) ampliprep
250	24-May-05	49,050	historic	cobas (Taqman) ampliprep

250	7-Jul-05	7,330	historic	cobas (Taqman) ampliprep
250	29-Sep-05	63,700	historic	cobas (Taqman) ampliprep
250	2-Mar-06	131,000	historic	cobas (Taqman) ampliprep
250	28-Jun-06	156,000	historic	cobas (Taqman) ampliprep
250	6-Sep-06	208,000	historic	cobas (Taqman) ampliprep
250	29-Nov-06	266,000	historic	cobas (Taqman) ampliprep
250	9-Jun-09	101,458	TI week 10	cobas (Taqman) ampliprep
250	16-Jul-09	78,853	TI week 14	cobas (Taqman) ampliprep
251	30-Mar-01	30,054	historic	cobas (Taqman) ampliprep
251	9-Jun-09	10,518	TI week 10	cobas (Taqman) ampliprep
251	16-Jul-09	22,639	TI week 14	cobas (Taqman) ampliprep
252	23-Oct-03	2,635	historic	cobas (Taqman) ampliprep
252	18-Dec-03	129,962	historic	cobas (Taqman) ampliprep
252	29-Jan-04	366,667	historic	cobas (Taqman) ampliprep
252	18-Mar-04	306,904	historic	cobas (Taqman) ampliprep
252	14-May-04	3,949	historic	cobas (Taqman) ampliprep
252	11-Aug-09	0	TI week 10	cobas (Taqman) ampliprep
252	8-Sep-09	0	TI week 14	cobas (Taqman) ampliprep

Table S3A. Absolute CD4 summaries and analysis for all subjects infused on the 6 dose protocol.

TMPT	Study Day	CD4 T Cell counts (cells per mm ³ of blood)														
		201	202	203	204	206	207	208	209	211	212	213	214	215	Avg	Std Dev
Screen	Screen	803	363	510	470	670	611	608	524	367	566	362	473	760	545	144
Week -2	Safety Labs	901	346	567	431	539	544	386	638	320	440	382	412	600	500	157
Day 0	Dose 1	867	384	481	304	565	441	428	537	269	524	404	368	700	482	163
Week 1	Safety Eval	637	436	563	553	513	592	336	576	328	530	466	467	769	520	119
Week 2	Dose 2	NA	NA	NA	NA	NA	NA	NA	NA	NA	NA	NA	NA	NA		
Week 3	Safety Eval	790	498	903	433	496	650	421	653	325	575	489	454	647	564	161
Week 4	Dose 3	NA	NA	NA	NA	NA	NA	NA	NA	NA	NA	NA	NA	NA		
Week 5	Safety Eval	934	593	651	573	514	817	364	698	420	773	645	411	793	630	173
Week 6	Safety Eval	812	560	654	457	617	533	535	391	383	720	484	408	610	551	130
Week 8	Safety Eval	1030	598	602	462	659	526	400	573	488	744	510	449	806	604	173
Week 9	Dose 4	888	447	661	496	481	507	490	618	432	580	535	NA**	696	569	130
Week 10	Safety Eval	1025	525	807	533	632	636	510	712	452	666	538	NA**	642	640	156
Week 11	Dose 5	1004	573	750	494	605	579	563	698	340	623	538	NA**	583	613	159
Week 12	Safety Eval	934	733	806	566	692	698	441	695	545	650	513	NA**	890	680	149
Week 13	Dose 6	890	661	769	538	718	486	421	570	390	920	548	NA**	927	653	191
Week 14	Safety Eval	903	660	689	447	547	553	393	888	476	681	Missed	340	875	621	195
Week 16	Safety Eval	944	677	990	508	712	611	426	762	464	690	Missed	442	1066	691	218
Week 18	STI	1022	656	606	548	573	620	506	566	295	797	NA	378	1029	633	223
Week 20	Safety Eval	832	551	671	456	622	196	NA	NA	NA	614	NA	345	956	583	233
Week 22	Safety Eval	677	317	550	337	180	576	NA	NA	NA	640	NA	297	1058	515	267
Week 24	Safety Eval	762	293	440	344*	352	631	576	542	453	522	719	271	708	522	166
Week 28	Safety Eval	697	257	462	381	485	691	NA	NA	NA	497	NA	366	571	490	147
Week 32	Safety Eval	730	354	447	394	480	688	NA	NA	NA	432	NA	372	629	503	142
Week 36	Safety Eval	636	435	463	301	601	613	576	646	533	579	567	440	388	521	106
Week 40	Safety Eval	686	350	403	347	681	571	NA	NA	NA	512	NA	350	797	522	171
Week 44	Safety Eval	711	455	542	304	782	Missed	NA	NA	NA	477	NA	381	947	575	219
Week 48	Safety Eval	602	473	468	307	684	591	NA	NA	NA	698	NA	380	913	568	185
Week 52	Safety Eval	687	464	465	356	599	632	604	668	391	612	653	427	627	553	115

CD4 T cell count values in **bold print** are those obtained while subject was not on ARVs

*CD4 count listed above for VRX496-204 for Week 24 is the average of two of two values: 318 (Week 24) and 370 (Week 24 REDRAW).

**Subject VRX496-214 did not have 2nd cycle of dosing of VRX496 (doses 4-6). QC testing of RCL by VIRxSYS, testing required and requested by the FDA delayed dose #4 by 6 weeks. In light of delay, team decided and protocol deviation approved to have subject proceed to STI after receiving 3 doses of VRX496 instead of 6 as stipulated in the protocol version in which subject was enrolled. Subject had Weeks 14 and 16 safety evaluations and then proceeded

Table S3B. Absolute CD4 summaries and analysis for all subjects infused on the 3 dose protocol.

Timepoint	Study Day	CD4 T Cell counts (cells per mm ³ of blood)					
		218	250	251	252	Avg	Std Dev
Screen	Screen	836	521	717	772	712	136
Week -2	Safety Labs	1060	418	703	896	769	276
Day 0	Dose 1	909	403	501	730	636	228
Week 1	Safety Eval	882	394	532	1422	808	458
Week 3	Safety Eval	947	563	1143	2156	1202	680
Week 5	Safety Eval	Missed	715	1044	2415	1391	902
Week 6	Safety Eval	881	424	944	2208	1114	765
Week 8	Safety Eval	898	409	867	2331	1126	834
Week 10	STI	760	452	774	2139	1031	753
Week 12	Safety Eval	817	599	718	1710	961	507
Week 14	Safety Eval	955	519	557	2083	1029	730
Week 16	Safety Eval	617	424	470	1442	738	476
Week 20	Safety Eval	627	350	450	1073	625	320
Week 24	Safety Eval	586	360	424	1274	661	420
Week 28	Safety Eval	704	391	400	1070	641	321
Week 32	Safety Eval	423	431	585	1178	654	357
Week 36	Safety Eval	426	311	607	935	570	272
Week 40	Safety Eval	510	306	584	869	567	233
Week 44	Safety Eval	519	354	587	Missed	487	120
Week 48	Safety Eval	Missed	360	626	Missed	493	188
Week 52	Safety Eval	732	178	670	938	630	322

CD4 T-cell count values in **bold print** are those obtained while subject was not on ARVs

2.1 Tables S4 and S5. Viral Evolution

2.1.1 Detailed description of viral evolution methods and results

To investigate antisense pressure, we considered only those post-ATI time-points after viral recrudescence and before patients restarted on ART. Successive time points assayed were separated by 4-8 weeks in an effort to capture possible viral signatures at any point during ATI.

For each patient we included the earliest time-point post-recrudescence available for analysis, because antisense pressure might be most detectable at the point of viral breakthrough. Virus was detectable in most patients by week 4 post-ATI. The earliest sample analyzed corresponded to week 6 (Table S4). Patient 201 was an exception as the earliest time-point available was for week 14. For patient 215, recrudescence was relatively delayed at 6 weeks but the earliest sample dated to 18 weeks. Patient 252 was of particular interest having suppressed virus at undetectable levels for 4 months post-STI and had a sample for week 18, which was when virus rebounded. All patient time-points studied, together with corresponding viral load and CD4 counts, are listed in **Table S4**.

We included as controls HIV-infected patients who participated in a ATI trial at the Wistar Institute, Philadelphia⁵¹ designed to evaluate effects of multiple intermittent treatment interruptions (TI). Participants were randomized into two cohorts. One group experienced three TIs of fixed term with intervening periods of ART resumption. Throughout this duration the other group underwent continuous ART. Both groups were then subject to an open-ended TI (OE-TI) before participants went back on ART.

For matched controls, longitudinal samples were obtained from nine patients from the OE-TI period. Similar to VRX496 patients, time-points selected for analysis were at least 4 weeks apart with the earliest being 4 or 8 weeks following OE-TI – except for patient 43, in which case the first available time-point was for week 14. Details for control samples including viral loads and CD4 counts are mentioned in **Table S5**. Patients 35 and 53 belonged to the group with continuous ART before OE-TI, whereas the rest were from the group with three TIs before OE-TI **[note: sequence data will be provided upon notification of acceptance]**.

Table S4. Patients on the VRX496 study and the time points post ATI evaluated for viral evolution.

Sample characteristics such as viral load and levels of VRX496-T are indicated along with Pyronoise OTU numbers recovered by denoising raw 454/Roche pyrosequence reads obtained for a given sample. TI: Treatment interruption; NA: Not available; NP: Not pyrosequenced due to insufficient DNA; 100*: Below limit of detection

ID	Visit date	Viral load (copies/ml)	CD4 (cells/ml)	Time post-TI (week)	VRX cells per 10 ⁶ PBMCs	Pyronoise OTUs
201	5/31/07	29520	730	14	1500	2663
201	6/28/07	28174	636	18	600	1815
201	8/23/07	18684	711	26	600	3760
201	10/18/07	33467	687	34	300	2719
201	12/13/07	16165	600	42	100	2756
203	8/9/07	39524	440	6	NA	4023
203	8/28/07	26925	462	10	300	2562
203	10/22/07	18463	463	18	200	243
203	12/20/07	8049	542	26	100	2199
203	2/14/08	26563	465	34	100*	2214
203	4/8/08	30982	462	42	100*	NP
204	11/5/07	26627	318	6	NA	1494
204	12/3/07	5993	381	10	300	2151
204	2/4/08	22108	301	18	100*	2337
204	3/31/08	20650	304	26	0	3901
204	5/22/08	16940	356	34	0	2900
215	6/11/09	3360	388	18	100	2958
215	8/6/09	4522	947	26	100	NP
215	10/13/09	3952	627	34	100	1744
215	12/16/09	3619	773	42	100	2148
218	6/18/09	97623	617	6	NA	3380
218	7/22/09	15497	627	10	100	2252

218	9/16/09	28061	704	18	100	249
218	11/11/09	24588	426	26	0	641
218	1/6/10	19508	519	34	NA	NP
250	5/12/09	414365	424	6	NA	6180
250	6/9/09	101458	350	10	300	3972
251	5/12/09	77545	470	6	NA	984
251	6/9/09	10518	450	10	500	NP
251	8/6/09	36921	400	18	300	580
252	10/6/09	5052	1070	18	1100	696
252	12/8/09	365196	935	26	500	4591

Table S5.-Matched controls⁵¹ and the time points post ATI which were evaluated for viral evolution.

Sample characteristics with viral load are indicated along with Pyronoise OTU numbers recovered by denoising raw 454/Roche pyrosequence reads obtained for a given sample. TI: Treatment interruption

ID	Visit date	Viral load (copies/ml)	CD4 (cells/ μ l)	Time post-TI (week)	Pyronoise OTUs
8	2/14/02	55812	352	4	2268
8	3/14/02	164904	228	8	1723
8	4/11/02	140203	234	12	4167
14	10/4/01	18961	858	4	1855
14	11/8/01	21246	574	9	2629
14	11/29/01	15197	694	12	1958
22	10/9/02	44673	893	4	1279
22	11/6/02	9943	953	8	1447
22	12/4/02	147500	966	12	1991
35	5/28/03	8621	464	8	1996
35	6/25/03	5291	393	12	1557
35	7/30/03	8921	318	17	2389
41	5/30/02	124747	661	8	1415
41	6/27/02	24995	467	12	1786
41	7/25/02	15464	533	16	2920
43	7/17/02	14424	496	14	1476
43	8/15/02	17247	409	18	3637
43	11/6/02	17531	488	30	2417
44	8/29/02	23519	341	4	2012
44	9/25/02	63255	362	8	2576
44	10/16/02	61417	279	11	3281
53	2/6/03	81957	531	4	2070

53	3/6/03	6572	701	8	1010
53	4/3/03	6152	630	12	1441
54	4/24/03	7860	747	4	3143
54	5/22/03	18581	644	8	2318
54	6/19/03	25870	636	12	2417

2.1.2 Viral RNA amplification and pyrosequencing

RNA was extracted from plasma samples for each patient/time-point combination listed in Tables S4 and S5. HIV RNA was reverse-transcribed and amplified following which PCR products were purified and pyrosequenced. The amplification was targeted to the region of *env* targeted by antisense (*envAS*) and involved a modification of the scheme described earlier.⁵² To take advantage of longer read lengths offered by the 454/Roche Titanium platform, the length of the two shorter *envAS* amplicons was increased. This also allowed inclusion of more positions outside the antisense-target region for comparison to targeted nucleotides. On the basis of earlier observations that antisense-mediated deletions were small (<100 bases),⁵² we anticipated that the two new *envAS* amplicons would be sufficient to detect antisense signatures, if any.

The current study required amplifying virus from different patients potentially with heterogeneous HIV sequence backgrounds. Under the assumption that patients harbored HIV subtype B, which is the predominant form in the USA, the new *envAS* primers were redesigned to sites of high conservation for HIV subtype B. This improved amplification efficiency for the patient samples as evidenced by gel electrophoresis. The coordinates of the *envAS* amplicons used in this study are illustrated in Figure 4A. For amplification, *envAS* primers were barcoded to enable multiplex pyrosequencing of samples.^{41,46} The 454/Roche microtiter sequencing plate can be physically separated into quadrants, which enabled recycling of barcodes 3-4 times over the sample set – barcode-primer combinations that performed best during testing were used more often. Complete primer sequences and their locations on VRX496 are cataloged in Figure 4A and Table S1.1.

Both *envAS* amplicons were pyrosequenced in two directions generating reads originating with either the forward or reverse primers in each case. After filtering for quality, a total of 218,756 pyrosequence reads were obtained over all patient/time-point and primer combinations. To remove sequencing errors, and cluster reads into unique viral variants – termed operational taxonomic units (OTUs) – the denoising algorithm Pyronoise was used.⁴³ This condensed the data into 127,290 OTUs over which further analysis was carried out. OTUs are enumerated according to sample in Tables S4 and S5. A few samples were not pooled for the pyrosequencing reaction due to undetectable DNA following amplification.

2.1.3 Framework to estimate A-G error rates and deletions

To determine enrichment for A-G transitions and deletions within the *envAS* target region, if any, it was important to carefully interpret base changes in the OTUs. For this, two things were necessary: 1) a reasonable multiple sequence alignment (MSA) wherein all OTUs would be lined up base-by-base, and 2) an appropriate reference sequence against which to measure base substitutions and deletions.

MSA for OTUs corresponding to each *envAS* primer was generated as described in previous work⁵² (also see Methods). One important difference was that to account for patient viral background heterogeneity in the *envAS* region, individual MSAs were first constructed for each patient. Also for the same reason, the majority OTU identified within a given patient was used to guide creation of these MSAs, rather than any standard reference. Next, all MSAs were brought in the context of HIV-1_{NL4-3}, which is the reference genome on which *envAS* is based. Subsequently, the *envAS* sequence was used to demarcate non-target and target bases for each read for each patient. A consensus was generated for each patient and used as the reference to help interpret changes in HIV sequences within a given patient. This was a reasonable approach to detect *envAS*-mediated effects, which were expected to be in a minority and thus potentially different from the consensus.

2.1.4 Preliminary assessment of A-G enrichment

As a first approach, an overall consensus sequence was created for each patient and for each *envAS* primer set from OTUs sampled over all time-points. The consensus was created two ways – by considering the frequency of isolation (or “weight”) of the OTUs, or not. We call this the weighted or un-weighted consensus respectively. Accordingly two modes of analysis were carried out: 1) weighted, at the level of total reads, by replicating each OTU as many times as its weight, and 2) un-weighted, at the level of OTUs, treating each OTU equally as if they had the same weight. The “de-replication” step condensing reads into unique viral variants corresponds to denoising and clustering of reads by Pyronoise.

Since we expect *envAS* effects to be in the minority, our anticipation was that these would show up better in the un-weighted analysis. For a given OTU, any base that was different from the consensus base at that position was characterized to be a base change. Base-change proportions per OTU were plotted for both VRX and control for all possible nucleotide substitutions. This was first done for the *envAS*-target region. Unlike that following HIV-1_{BaL} challenge in *envAS*-treated mice,⁵² we did not find outliers that were more enriched for A-G changes in the VRX patients compared to control patients (data not shown). G-A, which arises due to APOBEC action on HIV-1, was the highest overall as well as in terms of outliers in both groups – this recapitulates earlier findings⁵² and validates the approach of using the consensus to estimate nucleotide changes.

When pooled over groups, we found the proportion of OTUs enriched for A-G was higher in control patients at levels requiring a minimum of 5% or 10% change. Only at a level needing 15% or more A positions to change to G, relatively more OTUs were recorded in the VRX group. Closer inspection

revealed that patient 203 alone contributed approximately 95% of the numbers in the VRX group at this level. Thus, although there was some enrichment of OTUs with high A-G rates in the VRX group, effects were not equally strong in all patients. This is in contrast to that observed in the mouse study for the treated cohort challenged with HIV-1_{BaL}.⁵² To improve sensitivity, we restricted analysis for base changes to informative OTUs, which harbor at least one change of the given type. This did not lead to any further enrichment of OTUs in the VRX cohort at the different levels for A-G changes examined. A weighted analysis also did not enrich for A-G changes in VRX patients.

2.1.5 Alternative approaches to evaluate A-G changes

We considered the possibility that over time immune responses or residual drug effects in both groups of patients could lead to outgrowth of mutations at some sites at a high rate. These could add significant noise to the data while attempting to interpret the potentially more subtle changes due to *envAS*, making detection of such minority signatures difficult. Indeed, repeated base substitutions were observed longitudinally at a few sites while inspecting the MSAs. To account for this, we modified our analysis. A consensus was determined for each time-point, instead of a single consensus over all, and MSA positions where the majority base changed between time-points were discarded. As determined by Fisher's exact test (one-sided), this showed significant enrichment of OTUs in VRX patients at A-G change levels of 10% and 15% ($P < 10^{-12}$ and $P < 10^{-14}$ respectively) but not at 5% (data not shown). Statistical test was based on pooling of OTUs over all patients within each group and results were similar whether we considered all sequences or just informative ones. As earlier, patient 203 alone contributed a vast majority of the OTUs with high rates of A-G. As before, performing a weighted analysis did not improve signal detection and on the contrary, the enrichment observed at the 10% level was lost. For all further analysis, only the un-weighted approach was considered.

The earlier time-points sampled in VRX patients have the highest counts for VRX496-modified cells⁵³ (also see Figure 5). Modified cell levels fall over time in all patients. Also, once there is viral breakthrough, the expectation is that the fittest forms will gradually dominate the HIV quasi-species with time under given conditions. For these reasons, it is reasonable to expect *envAS* effects to be present and most readily detectable only toward the beginning of the post-STI period at the point of recrudescence. We therefore repeated all analysis by considering only the first time-point for all patients. To estimate changes, in addition to an overall consensus like earlier, we also considered a "founder" consensus built from OTUs detected in the first time-point.

As a consequence of custom filtering during the pyrosequence data acquisition step, error increases in the 3' bases of reads. This could confound estimates of true base changes, especially those generated in low frequencies. To account for this, we duplicated all analyses for the *envAS*-target region as before except considering only the first 100, and then the first 50, 5' positions for the MSAs for each primer set. This restricts analysis to increasingly high quality regions of the reads.

When considering high quality bases and constraining analysis to the first time-point and using founder consensus for interpreting changes, we found enrichment of OTUs in the VRX group by Fisher's exact test at all A-G change levels examined ($P < 10^{-5}$ at 15%, $P < 10^{-67}$ at 10%, and $P < 10^{-41}$ at 5%). This was not the case with other base changes. Importantly, we found a significant increase in numbers of OTUs with A-G among the VRX patients as estimated by Mann-Whitney test. ($P = 0.114$ at 10% and $P = 0.046$ at 5%). Enrichment of OTUs in VRX patients at the 5% level as determined by Mann-Whitney test for all base changes is given in Figure S1A. Apart from evidence of the A-G effect in the initial time-point, we also recorded significant excess of OTUs with G-C substitutions for the third time-point. The G-C enrichment, however, did not survive the correction with non-target region substitution rates as described below.

(A)

Within Antisense

		To						To			
		1	A	T	G	C	3	A	T	G	C
From	A			0.760	0.046	0.405			0.523	0.697	0.703
	T	0.977			0.240	0.629	0.772		0.864	0.772	
	G	0.697	0.212			0.240	0.836	0.344		0.025	
	C	0.519	0.593	0.407			0.994	0.568	0.736		
		2	A	T	G	C	All	A	T	G	C
From	A			0.568	0.568	0.303			0.593	0.336	0.371
	T	0.568			0.967	0.612	0.970		0.882	0.593	
	G	0.836	0.164			0.612	0.697	0.407		0.100	
	C	0.772	0.656	0.736			0.815	0.444	0.629		

(B)

Rate Differentials

		To						To			
		1	A	T	G	C	3	A	T	G	C
From	A			0.556	0.057	0.084			0.344	0.264	0.388
	T	0.271			0.729	0.336	0.344		0.772	0.523	
	G	0.084	0.729			0.629	0.164	0.998		0.388	
	C	0.444	0.729	0.118			0.836	0.344	0.432		
		2	A	T	G	C	All	A	T	G	C
From	A			0.736	0.432	0.344			0.371	0.212	0.185
	T	0.612			0.943	0.568	0.556		0.882	0.444	
	G	0.523	0.388			0.697	0.303	0.697		0.444	
	C	0.836	0.982	0.112			0.729	0.556	0.185		

Figure S1. P values for enrichment of base changes in *envAS* target region among VRX patients.

(A) Enrichment in VRX patients of OTUs containing at least 5% base changes within the *envAS* target region. (B) Significant excess of rate differentials in VRX patients. For each nucleotide substitution, the difference in rates between target and non-target parts was determined per patient. In both A and B,

Mann-Whitney P values are listed. Analysis was performed separately for time-points 1-3 and for all time-points pooled. Time-points are indicated in a shaded box to the upper left of each panel. Significant P values, or that closest to significance as in **(B)**, are highlighted by white lettering.

2.1.6 Base change comparisons between *envAS* target and non-target regions

Given the above trend for A-G transitions, we investigated if normalizing against changes in the non-target region could reinforce this signal. Earlier work had reported preferential *envAS*-mediated A-G transitions in the *envAS*-target as opposed to the adjoining non-target region.^{52,54} For the current study we designed our amplicons to include 240 adjacent non-target bases (with a variation of a few bases across patients) – 150 to the left and 90 to the right of the 937 base long *envAS*-target region (Figure 4A). This made it feasible to interrogate whether comparisons of nucleotide substitution rates within patients between target and non-target parts might bolster the A-G signal in the VRX group.

We repeated the analysis described in previous sections for the non-target regions. Although A-G rates varied across patients, there was no evidence of any difference between the control and VRX groups by Mann-Whitney test. We proceeded to calculate differences in target and non-target region base change rates. First, we identified appropriate nucleotide positions for this analysis such that non-target and target bases would be matched for quality. This was relevant as the A-G effect best showed up when restricting analysis to higher quality bases in the target region. The custom filtering performed during sequence data recovery from the 454/Roche sequencer yields high quality bases for the first ~175-200 5' positions in the direction of sequencing with errors increasing further 3'. For each *envAS* primer set, we selected the first 200 5' positions.

Over all 4 *envAS* primer sets, we thus considered 800 nucleotide positions. These included all 240 non-target positions amplified and 560 target positions. We compared to the founder consensus to determine base changes. Base change rates were calculated separately for target and non-target parts for each patient. By taking the difference in rates between the two parts, we estimated relative base changes in the target region. This was done over all possible base changes.

Our hypothesis was that A-G rate excess would be more in the VRX group, so we performed a one-sided Mann-Whitney test to check for higher A-G rate differentials among VRX patients, which yielded $P = 0.057$ for the first time-points (**Figure S1B**). This trend for A-G was not detectable for other time-points or when all time-points were pooled. Notably, no other base change recorded a higher significance across any time-points (**Figure S1B**). The distribution of rate differentials for the first time-point for all base changes is shown in **Figure S2**.

We repeated our analysis by considering the first 250 5' positions for each *envAS* primer set. This gave a total of 1000 nucleotide positions – 240 of them non-target and 760 target. Within the target parts, Fisher's test revealed OTU enrichment at different levels of A-G turnover for the initial time-point as

before. Also like previously, Mann-Whitney test indicated significance across all patients at low levels of A-G transitions (1-2%). Testing for rate differentials between target and non-target parts preserved the trend for A-G in VRX patients for the initial time-point ($P = 0.069$; Mann-Whitney test – data not shown). Again, this effect was not visible for any other time-point. This reproduces observations recorded earlier in this section with a different selection for high quality bases. Thus we find an indication of possible *envAS*-induced A-G transitions in this study.

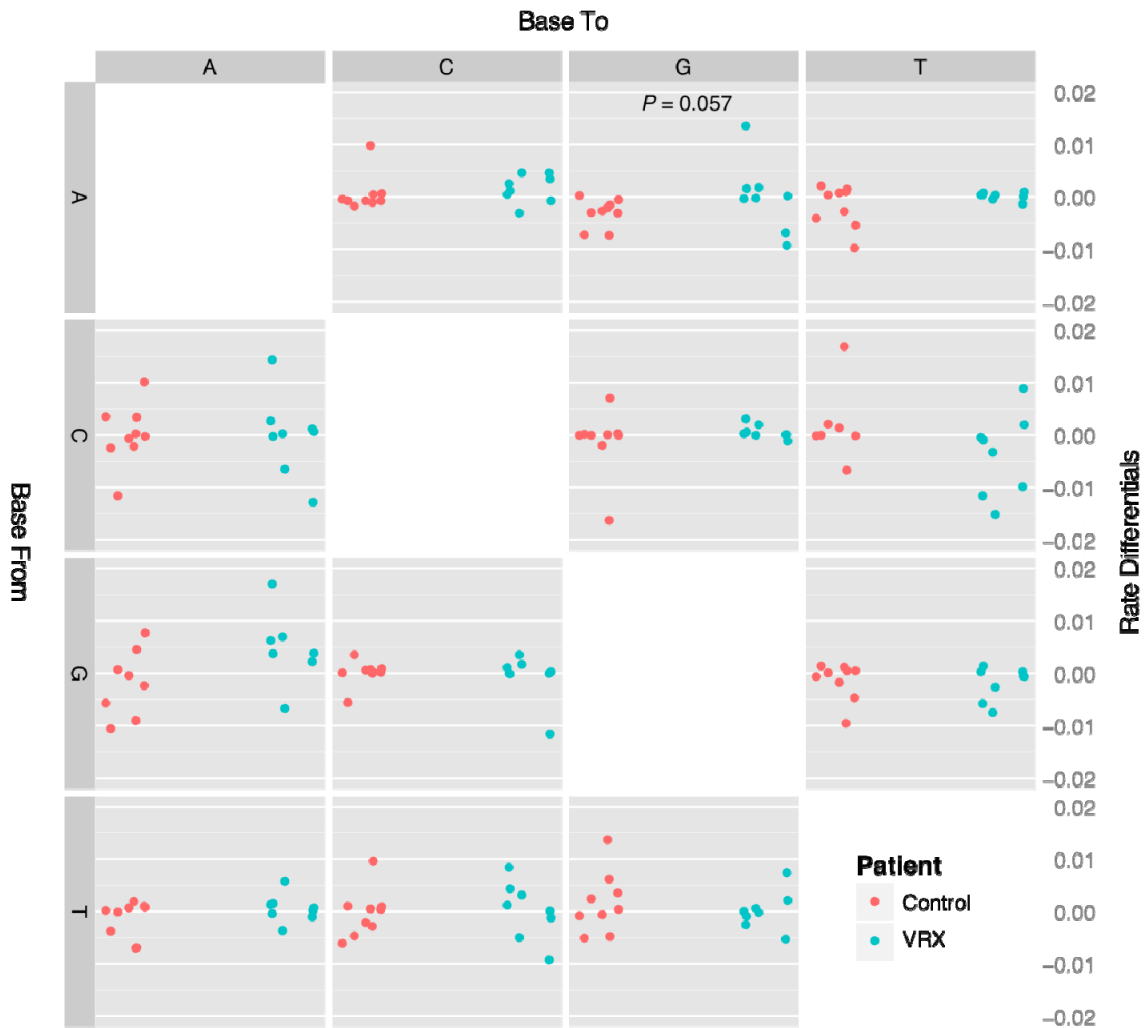


Figure S2. Differences in rates between *envAS* target and non-target parts for each base change per patient.

All possible base changes are shown. For A-G changes, there is a near significant trend for higher rate differentials among VRX patients compared to controls (see the panel for Base From 'A' and Base To 'G'). Two outliers each for G-A and C-T panels have been removed for visualization purposes.

2.1.7 Distribution of deletions

We next analyzed if *envAS* also led to higher numbers of target region deletions in viral populations among VRX patients. On similar lines as the A-G analysis, we identified deletions with the help of founder consensus and using criteria for deletions as defined in the mouse study. The distribution of variants with deletions is shown in **Figure S3**. We did detect enrichment for deletion-bearing sequences in the VRX group ($P < 10^{-6}$; Fisher's exact test, one-sided), however all VRX patients did not support this ($P = 0.44$; Mann-Whitney test, one-sided). Also, in contrast to the A-G effect, there was no excess of deletions in VRX group when only the initial time-points were evaluated by Fisher's test.

Researchers studying *envAS* pressure in tissue culture reported high proportion of variants containing deletions in the target region while analyzing breakthrough virus.⁵⁴ We considered the possibility that unlike A-G effects, deletions might not be a minority signature. In this case, deletions in breakthrough variants could be reflected in founder consensus making it less useful in interpreting missing bases. Therefore all analysis was repeated using an overall consensus. This yielded significance over OTUs from all time-points pooled as well as for the first time-point separately ($P < 10^{-64}$ and $P < 10^{-21}$ respectively; Fisher's test). Still, Mann-Whitney test failed to support enrichment for deletions over all VRX patients in the per subject analysis. Performing a weighted analysis either with founder or overall consensus did not change findings. We thus conclude that evidence for deletions was not as robust as for A-G transitions, and was likely anecdotal in a few VRX patients, primarily VRX201.

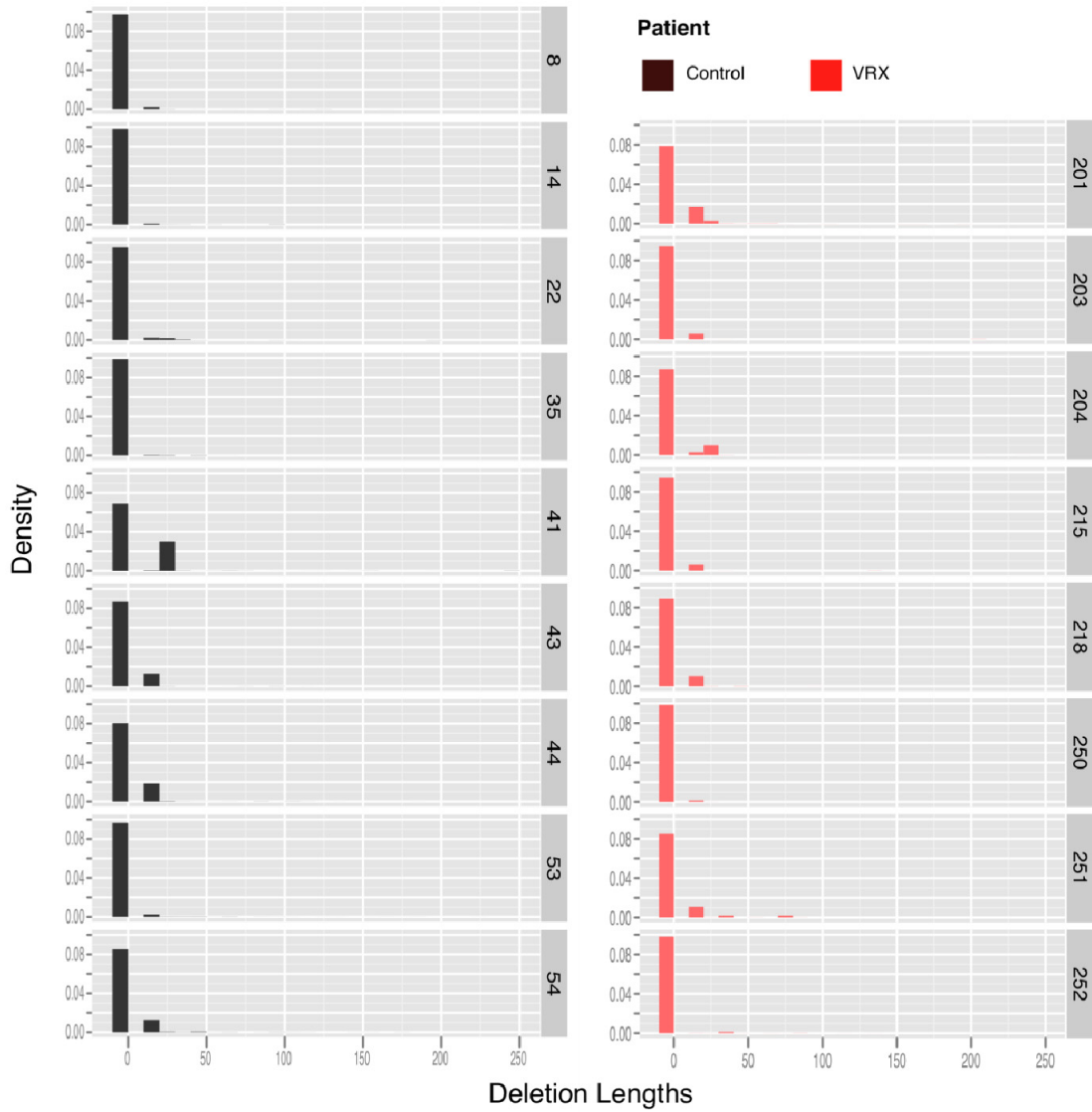


Figure S3. Histogram of OTUs binned by total deletion lengths.

Relative proportions, indicated by density along the y-axis, are plotted for a bin size of 10. Thus proportion OTUs in each bar corresponds to density*10. Tall bars to the left of 0 represent OTUs lacking deletions. Distributions shown are over all time-points.

Table S6A. Persistence of Vector-Modified Cells in subjects enrolled under 6 dose Protocol.

Timept	Study Day	Persistence of Vector-Modified Cells (copies per 1x 10 ⁶ PBMC)												
		201	202	203	204	206	207	208	209	211	212	213	214	215
Screen	Screen	NA	NA	NA	NA	NA	NA	NA	NA	NA	NA	NA	NA	NA
Week -2	Safety Labs	NA	NA	NA	NA	NA	NA	NA	NA	NA	NA	NA	NA	NA
Day 0	Dose 1	0	0	sample lost	0	0	0	0	0	0	0	0	0	0
Week 1	Safety	5500	12100	34900	20700	18400	25200	36300	23200	7000	10500	11500	1800	33000
Week 2	Dose 2	1500	4500	3300	25900	13800	5500	invalid	14700	3800	2700	700	1300	24600
Week 3	Safety	12500	4500	3700	45100	16500	2600	600	13900	12000	5700	600	2000	2800
Week 4	Dose 3	7700	4000	1200	59000	6000	500	100	7600	3900	4000	300	500	400
Week 5	Safety	9000	4100	1500	22600	1000	1400	100	1600	900	5300	900	100	300
Week 6	Safety	5300	2200	1400	2500	200	600	0	600	100	1100	*100	0	200
Week 8	Safety	13400	1400	400	700	800	1000	0	600	100	1400	*100	*100	200
Week 9	Dose 4	6900	900	200	700	300	400	0	400	100	800	*100	NA	300
Week 10	Safety	10700	1200	700	900	400	1200	300	600	300	2900	*200	NA	300
Week 11	Dose 5	12300	800	500	400	300	500	1500	300	0	3400	*100	NA	200
Week 12	Safety	15300	600	800	400	400	1600	100	700	*100	7700	*100	NA	700
Week 13	Dose 6	12500	200	1700	400	300	1000	100	200	0	1700	100	NA	400
Week 14	Safety	7800	1100	600	200	300	600	0	300	*100	5900	Missed	0	300
Week 16	Safety	9800	400	300	300	400	400	0	*100	0	1400	Missed	0	200
Week 18	STI	2000	1000	500	300	900	200	100	*100	0	1200	NA	200	100
Week 20	Safety	2300	400	800	200	400	100	NA	NA	NA	3100	NA	0	100
Week 22	Safety	1500	100	200	100	100	100	NA	NA	NA	1500	NA	0	200
Week 24	Safety	800	NA	NA	NA	NA	NA	0	*100	0	NA	Not Done	NA	NA
Week 28	Safety	NA	100	300	300	100	300	NA	NA	NA	300	NA	0	100
Week 32	Safety	1500	NA	NA	NA	NA	NA	NA	NA	NA	NA	NA	NA	NA
Week 36	Safety	600	300	200	*100	*100	100	*100	0	0	300	0	0*	100
Week 40	Safety	NA	NA	NA	NA	NA	NA	NA	NA	NA	NA	NA	NA	NA
Week 44	Safety	600	200	100	0	*100	Missed	NA	NA	NA	500	NA	0	100
Week 48	Safety	NA	NA	NA	NA	NA	NA	NA	NA	NA	NA	NA	NA	NA
Week 52	Safety	300	400	*100	0	100	100	ND	0	0	400	100	0	100

A VRX496 transduced t-cell count (persistence of vector-modified cells) test was done for VRX496-201 on Weeks 24 and 32 although the test is not scheduled for those visits. For the other subjects proceeding to Step 2, the test was not be done on those weeks; it was done according to the protocol schedule of study procedures (wks 28, 36, 44, 52, 60, 68 & follow-up visits).

VRX496-208 did not proceed to Step 2; therefore, a VRX496 transduced t-cell ct was done for that subject on Week 24, per protocol. The VRX496 transduced t-cell ct test will not be done for this subject on Weeks 28, 32 & 36.

**Subject VRX496-214 did not have 2nd cycle of dosing of VRX496 (doses 4-6). QC testing of RCL by VIRxSYS, testing required and requested by the FDA delayed dose #4 by 6 weeks. In light of delay, team decided and protocol deviation approved to have subject proceed to STI after receiving 3 doses of VRX496 instead of 6 as stipulated in the protocol version in which subject was enrolled. Subject had Weeks 14 and 16 safety evaluations and then proceeded to Week 18, STI.

Table S6B. Persistence of vector-modified cells in subjects enrolled under 3 dose protocol.

Timepoint	Study Day	Persistence of VRX496 Modified Cells (copies per 1 x 10 ⁶ PBMC)			
		218	250	251	252
Screen	Screen	NA	NA	NA	NA
Week -2	Safety Labs	NA	NA	NA	NA
Day 0	Dose 1	0	0	0	0
Week 1	Safety Eval	2500	23500	19300	120800
Week 2	Dose 2	1300	11400	49600	106800
Week 3	Safety Eval	600	13300	100200	133700
Week 4	Dose 3	200	11200	92700	31400
Week 5	Safety Eval	Missed	14800	186800	31200
Week 6	Safety Eval	200	6400	51900	17000
Week 8	Safety Eval	200	1300	18400	8600
Week 10	STI	100	1600	5400	8200
Week 12	Safety Eval	100	1300	2600	4400
Week 14	Safety Eval	100	1500	900	4400
Week 16	Safety Eval	NA	NA	NA	NA
Week 20	Safety Eval	100	300	500	1900
Week 24	Safety Eval	NA	NA	NA	NA
Week 28	Safety Eval	100	300	300	1100
Week 32	Safety Eval	NA	NA	NA	NA
Week 36	Safety Eval	0	200	200	500
Week 40	Safety Eval	NA	NA	NA	NA
Week 44	Safety Eval	ND	200	500	Missed
Week 48	Safety Eval	Missed	NA	NA	Missed
Week 52	Safety Eval	0	0	200	1000

Values in **bold** print were obtained while subject was not on ARVs.

Table S7. VRX496-T persistence in peripheral blood and GALT. Shown are the log₁₀ of the total numbers of VRX496-T per million cells (total) or per 10,000 CD4 T cells (CD4). Patient numbers are shown, followed by the biopsy identified as 1, 2, 3, or 4 as shown in order of collection in Figure 1.

Patient-biopsy	total PBMC	total IEL	CD4 PBMC	CD4 IEL	Patient-biopsy	total PBMC	total IEL	CD4 PBMC	CD4 IEL
201-1					209-1		1		2
201-2	3.95	4.27	4.33	5.04	209-2	3.2	2.88	3.61	4.12
201-3	3.99	3.26	4.32		209-3	1	1	2	2
201-4	2.9	2.48	3.33	3.35	209-4	1	1	2	2
202-1					211-1		1		2
202-2	3.34	3.28	3.79	4.55	211-2	2	2.66	2.81	3.65
202-3	3.04	2.43	3.43		211-3	1	1	2	2
202-4	2	1	2.75	2	211-4	1	1	2	2
203-1		1		2	212-1		1		2
203-2	2.6	3.01	3.1	3.84	212-2	3.04		3.57	
203-3	2.48	2.97	2.9	3.72	212-3	3.77	3.11	4.33	4.01
203-4	2.4	2.54	3.14	3.19	212-4	2.95	2.27	3.69	3.11
204-1		1		2	213-1		1		2
204-2	3.4	3.11	3.87	4	213-2	1	1	2	2
204-3	2.48	2.02	3	2.58	214-1		1		2
204-4	2.3	1	2.86	2	214-4	1	1	2	2
206-1		1		2	218-1		1		2
206-2	2.3		2.94		218-2	2.3	2.2	2.87	3.13
206-3	2.6	1	3.13		218-3	2	1	2.73	2
206-4	2		2.64		250-2	3.11	1	3.94	2
207-1		1		2	250-3	2.95	1	3.84	2
207-2	3	2.87	3.63	3.56	251-1		1		2
207-3	2.78	2.73	3.42	3.53	251-2	4.26	2.92	4.72	4.19
207-4	2.3		3.02		251-3	2.85	1	3.56	2
208-1		1		2	252-1		1		2
208-2	1	1	2	2	252-2	4.23	2.53	4.72	3.71
208-3	1		2		252-3	3.5	1	3.79	2

Table S8. Integration Site Data

Supplementary Table S8(A). Clonal Abundance Estimation Using Independent Mu Integrations. Integration sites from abundant cell clones will be present at a higher frequency compared to sites from less abundant cells, allowing Mu to independently recover sites from abundant clones more often. Due to Mu's near-random integration of PCR adapters, it is unlikely that MuA transposase will deposit adapters more than once at the same genomic position in any given sample. Thus, the number of uniquely positioned Mu-deposited linkers recovering the same integration site provides an estimate of the abundance of vector-modified cells. This table shows the only sites recovered independently more than twice by Mu.

Patient	Timepoint	Chromosome	Orientation	Nucleotide Position	muttops	NearestRefSeq	NearestRefSeqDist	NearestOncoDist	Gene Function
251	week 6	chr14	-	71103417	18	SIPA1L1	0	2144821	(PMID: 15778465); Bound by the HPV E6 oncoprotein, binding leads to SIPA1L1 degradation (PMID: 16999984); Potential interactor with deubiquitinating enzymes (PMID: 19615732); as a tumor suppressor inhibiting PI3K signaling (PMID: 19647222)
250	week 6	chr4	-	143339689	15	INPP4B	0	985830	(PMID: 19647222)
252	week 6	chr18	-	19895289	13	TTC39C	0	1000596	Unknown

Supplementary Table S8(B). Unique Integration Sites Recovered per Patient and Timepoint. Patient numbers are shown above table columns. Rows show vector copy numbers per million PBMC and number of unique sites for each timepoint.

Patient	204		212		250		251		252	
	Copy Num. *	Unique sites	Copy Num. *	Unique sites	Copy Num. *	Unique sites	Copy Num. *	Unique sites	Copy Num. *	Unique sites
Preinfusion	1.9e10 ⁶	6812	7e10 ⁵	4507	1.1e10 ⁶	4209	9e10 ⁵	4959	6e10 ⁵	2764
Week 6	2500	18	1100	127	6400	48	51900	285	17000	308
Week14 or 16	200	4	5900	162	NA	3	NA	0	NA	55
Week 24	NA	0	NA	28	-	-	-	-	-	-
Total unique sites		6834		4824		4260		5244		3127

* Vector copy number per 10⁶ PBMC

2.2 Safety and immunogenicity of VRX496-T

RCL testing was performed in accordance with current FDA Guidance for RCR testing. Seven vector lots were used in cell manufacture and all were negative for RCL by biologic assay. A biologic RCL assay was not required on each cell product, since qPCR-based assays showed no RCL was amplified during the culture process due the addition of anti-retroviral drugs in the culture. Each cell product was tested for vector packaging DNA (VSV-G) to test for residual vector packaging DNA and RCL generation prior to release.

Patients were monitored quarterly for potential vector-derived RCL through PBMC analysis for VSV-G DNA since HIV derived DNA sequences would not be informative in this HIV+ population. VSV is an RNA based virus, and therefore detection of a VSV-G DNA would indicate a recombinant event with the packaging DNA. All patients had no evidence of RCL in the first year, and subsequent annual samples are collected and archived.

Notably, although RCL was negative, approximately 50% (7/13) of patients tested became seropositive to VSV-G. This is thought to be a response to residual levels of VSV-G protein on the final cell product (**Table S9**), which was too low to be detected in flow based assays (not shown). VSV-G antibody positivity did not correlate with VRX496-T persistence, and no infusion reactions occurred in patients with positive serology.

Table S9. VSV-G antibody detection summary (immunogenicity)

Tmpt	Results by Patient (P=Positive, N=Negative, ND=Not Done)																		Pos	Neg	Not Done
	201	202	203	204	206	207	208	209	211	212	213	214	215	218	250	251	252				
Screen	N	N	N	N	N	N	N	N	N	N	N	N	N	N	N	N	N	0/17	17/17	0/17	
wk 5	NA	NA	P	NA	NA	NA	NA	NA	NA	NA	NA	NA	NA	NA	NA	NA	NA	1-Jan	0	0	
wk 6	NA	NA	P	NA	NA	NA	NA	NA	NA	NA	NA	NA	NA	NA	NA	NA	NA	1-Jan	0	0	
wk 8	N	N	P	N	N	N	N	N	N	N	N	N	P	ND*	ND*	ND*	ND*	13-Feb	13-Nov	4	
wk 9	NA	NA	NA	P	NA	NA	NA	NA	NA	NA	NA	NA	NA	NA	NA	NA	NA	1-Jan	0	0	
wk 10	NA	P	NA	P	NA	P	NA	NA	NA	NA	NA	NA	NA	NA	NA	NA	NA	3-Mar	0	0	
wk 11	NA	P	NA	P	NA	P	P	NA	NA	NA	NA	NA	NA	NA	NA	NA	NA	4-Apr	0	0	
wk 12	NA	P	NA	P	NA	P	P	NA	NA	NA	NA	NA	NA	NA	NA	NA	NA	4-Apr	0	0	
wk 13	NA	P	NA	P	NA	P	P	NA	NA	NA	NA	NA	NA	NA	NA	NA	NA	4-Apr	0	0	
wk 14	N	P	P	P	N	P	P	N	P	N	missed visit	N	ND*	NA	NA	NA	NA	11-Jun	11-May	2	
wk 16	N	P	P	P	N	P	P	N	P	N	missed visit	N	ND*	NA	NA	NA	NA	11-Jun	11-May	2	
wk 52	N	P	P	P	N	P	ND*	N	P	N	ND*	ND*	ND*					9-May	9-Apr	4	

*Kits for performing assay no longer available; therefore, VIRxSYS not able to process and provide results for test.

Table S10. Summary of anti-HIV immune responses in patient PBMC pre- and approximately 10 weeks post-ATI

Patient	PBMC	%CD3+		% degranulation in CD3+ cells				% cytokine production in CD3+ cells			
		CD8+	CD4+	P/I*	non-infected	VRX1169-Infected	Ratio Infected/uninfected	P/I	non-infected	VRX1169-Infected	Ratio Infected/uninfected
201	pre	27.4	31.5	46.2	0.4	0.5	1.3	14.8	1.4	2.9	2.1
	post	22.1	26.7	40.8	0.7	0.7	1.0	17.1	3.1	2.5	0.8
250	pre	17.9	17.7	4.2	1.9	1.3	0.7	27.8	0.9	2.5	2.8
	post	41.2	10.1	21.2	2.9	2.8	1.0	13.2	1.0	2.5	2.5
251	pre	28.1	37.2	24.1	0.7	0.7	1.0	24.1	2.2	0.5	0.2
	post	41.0	10.2	12.8	0.7	0.7	1.0	11.9	4.4	2.2	0.5
252	pre	6.0	5.7	6.7	1.7	1.3	0.8	23.0	0.7	2.0	2.9
	post	20.9	5.6	29.0	2.6	1.8	0.7	10.5	0.8	2.0	2.5
215	pre	28.1	31.0	25.6	1.1	1.1	1.0	24.5	2.3	0.6	0.3
	post	22.8	26.3	13.5	1.0	1.0	1.0	12.6	4.9	2.6	0.5
218	pre	not done	not done	74.2	1.3	1.5	1.2	41.6	1.8	5.8	3.2
	post	not done	not done	47.7	1.2	3.2	2.7	23.8	3.0	3.5	1.2

*PMA and ionomycin stimulation

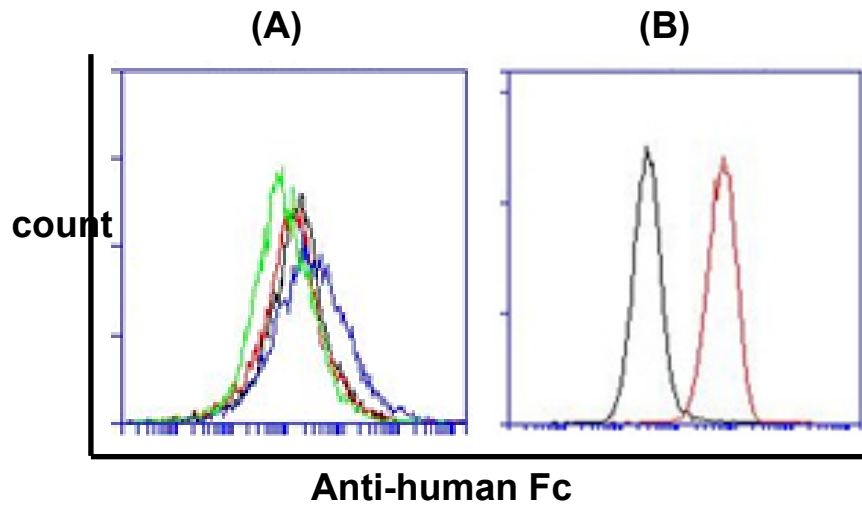


Figure S4. Absence of humoral immune responses directed against gene-modified cell product.

Data are from flow-cytometry-based assays performed essentially as described.⁵⁵ For these analyses, infusion product was incubated with dilutions of plasma (1:10, 1:20, 1:100) obtained from patients prior to-, at-, or approximately 10 weeks post- STI, and antibodies in plasma samples directed against the infusion product were detected using a FITC conjugated AffiniPure F(ab')₂ fragment goat anti-human IgG, Fcγ fragment specific reagent (Jackson ImmunoResearch, cat# 109-096-008). Data are presented for the 1:10 dilution of PT218 samples, and are representative of data obtained for patients 201, 204, 251, and 252 at all dilutions. Data presented are gated on live cells. (A): Analysis of patient 218 samples; Green line: secondary alone, black line: Pre-infusion sample; red line: STI sample; blue line: Post STI sample. (B): Detection of surface Fc on control cells: staining of immortalized B cell line (B-LCL, surface positive for human Fc receptor). Black line: no stain, red line: secondary reagent

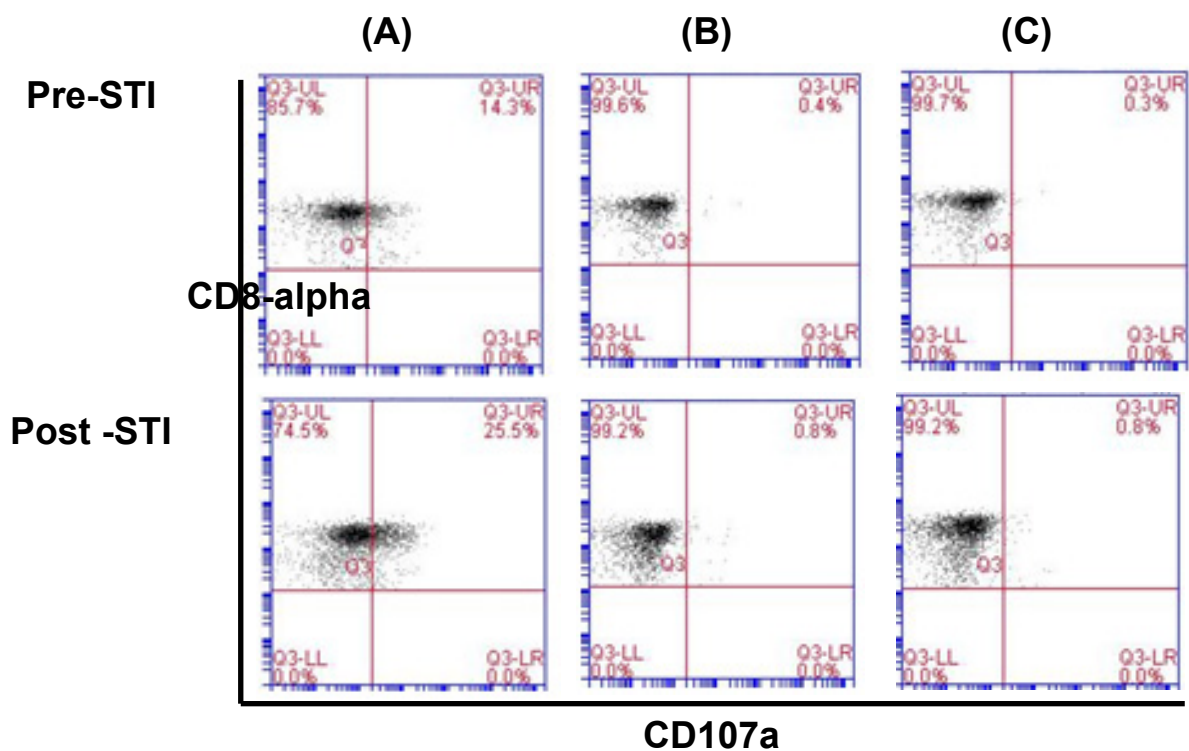


Figure S5. Absence of cellular immune responses directed against gene-modified cell product.

Data are from CD107 degranulation assays performed essentially as described.⁵⁶ For these analyses, effector cells (patient PBMC collected pre- or post- STI) were incubated with PMA/ionomycin (panel A) without infusion product (panel B), or with CFSE-labeled infusion product (panel C). The gating strategy involved sequential gating as follows: Live cells>CFSE-negative cells>CD3+>CD8+. Data are presented for PT218 samples, and are representative of data obtained for patients 201, 204, 251, and 252.

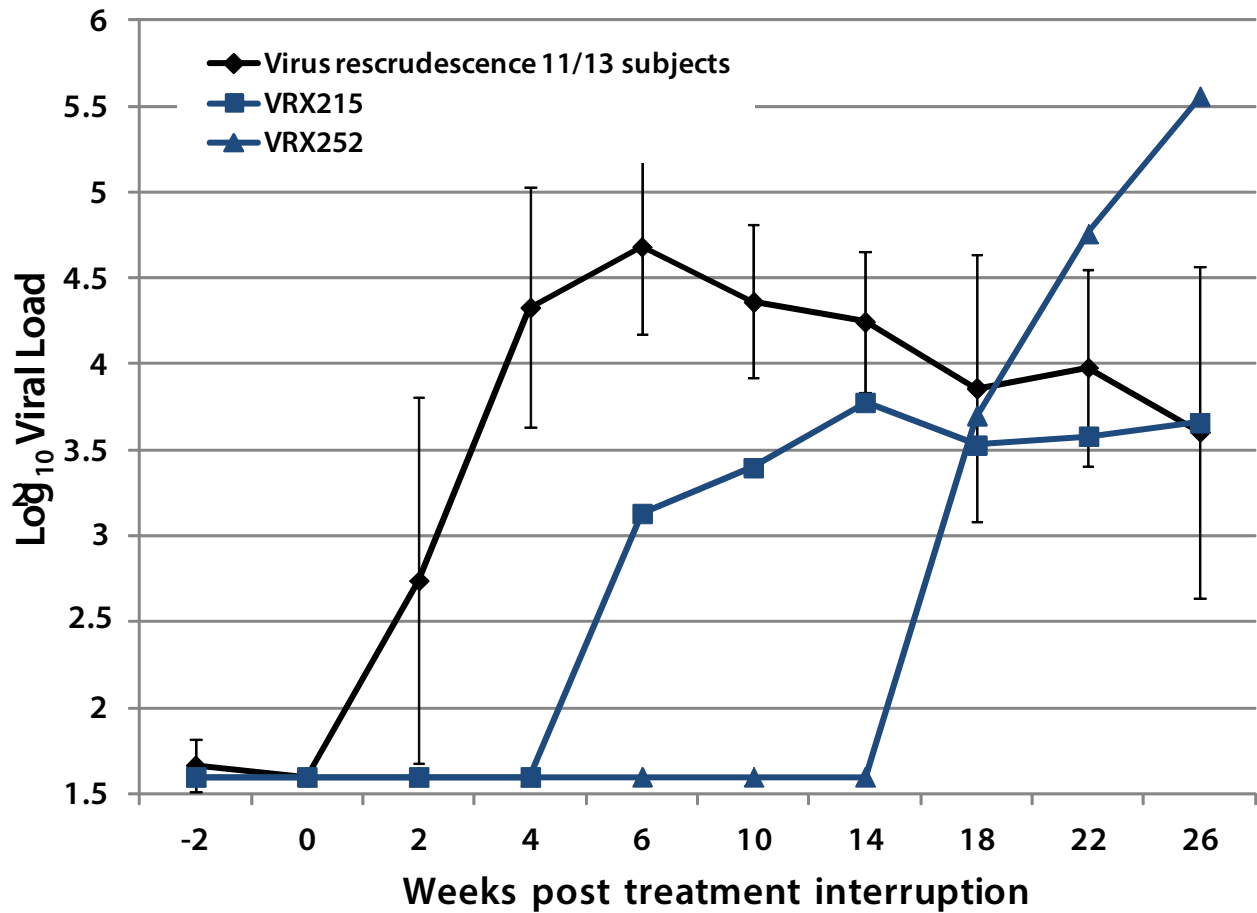


Figure S6. Effects of VRX496-T on HIV-1 viral load.

Virus recrudescence post ATI is shown for the 13 evaluable patients. The geometric mean values are shown for 11 of the 13 subjects. Subjects 215 and 252 broken out separately to show their delay in viral recrudescence. Error bars represent standard deviation, and data is censored once patients resume ARV. Patient 215 remained on ATI at 1 year, and 252 resumed ARV at week 44 due to a viral load >100,000.

Supplemental References

40. Hoffmann C, Minkah N, Leipzig J, et al. DNA bar coding and pyrosequencing to identify rare HIV drug resistance mutations. *Nucleic acids research*. 2007;35(13):e91.
41. Binladen J, Gilbert MT, Bollback JP, et al. The use of coded PCR primers enables high-throughput sequencing of multiple homolog amplification products by 454 parallel sequencing. *PLoS ONE*. 2007;2(2):e197.
42. Quince C, Lanzén A, Curtis TP, et al. Accurate determination of microbial diversity from 454 pyrosequencing data. *Nature methods*. 2009;6(9):639-641.
43. Reeder J, Knight R. Rapid denoising of pyrosequencing amplicon data: exploiting the rank-abundance distribution. *Nature methods*. 2010;7(9):668.
44. Brady T, Roth SL, Malani N, et al. A method to sequence and quantify DNA integration for monitoring outcome in gene therapy. *Nucleic Acids Res*. 2011;39(11):e72.
45. Wang GP, Levine BL, Binder GK, et al. Analysis of lentiviral vector integration in HIV+ study subjects receiving autologous infusions of gene modified CD4+ T cells. *Mol Ther*. 2009;17(5):844-850.
46. Hoffmann C, Minkah N, Leipzig J, et al. DNA bar coding and pyrosequencing to identify rare HIV drug resistance mutations. *Nucleic Acids Res*. 2007;35(13):e91.
47. Berry C, Hannenhalli S, Leipzig J, Bushman FD. Selection of target sites for mobile DNA integration in the human genome. *PLoS Comput Biol*. 2006;2(11):e157.
48. Brady T, Agosto LM, Malani N, Berry CC, O'Doherty U, Bushman F. HIV integration site distributions in resting and activated CD4+ T cells infected in culture. *Aids*. 2009;23(12):1461-1471.
49. Wang GP, Ciuffi A, Leipzig J, Berry CC, Bushman FD. HIV integration site selection: analysis by massively parallel pyrosequencing reveals association with epigenetic modifications. *Genome Res*. 2007;17(8):1186-1194.
50. Shacklett BL, Yang O, Hausner MA, et al. Optimization of methods to assess human mucosal T-cell responses to HIV infection. *Journal of Immunological Methods*. 2003;279(1-2):17-31.
51. Papasavvas E, Kostman JR, Mounzer K, et al. Randomized, controlled trial of therapy interruption in chronic HIV-1 infection. *PLoS medicine*. 2004;1(3):e64.
52. Mukherjee R, Plesa G, Sherrill-Mix S, Richardson MW, Riley JL, Bushman FD. HIV Sequence Variation Associated With env Antisense Adoptive T-cell Therapy in the hNSG Mouse Model. *Mol Ther*. 2010;18(4):803-811.
53. Levine BL, Humeau LM, Boyer J, et al. Gene transfer in humans using a conditionally replicating lentiviral vector. *Proceedings of the National Academy of Sciences of the United States of America*. 2006;103(46):17372-17377.
54. Lu X, Yu Q, Binder GK, et al. Antisense-mediated inhibition of human immunodeficiency virus (HIV) replication by use of an HIV type 1-based vector results in severely attenuated mutants incapable of developing resistance. *J Virol*. 2004;78(13):7079-7088.
55. Jensen M, Popplewell L, Cooper L, et al. Anti-transgene rejection responses contribute to attenuated persistence of adoptively transferred CD20/CD19-specific chimeric antigen receptor re-directed T cells in humans. *Biology of Blood and Marrow Transplantation*. 2010;16(9):1245-1256.
56. Cao LF, Krymskaya L, Tran V, et al. Development and application of a multiplexable flow cytometry-based assay to quantify cell-mediated cytolysis. *Cytometry A*. 2010;77(6):534-545.